arXiv:1512.06587v3 [hep-ph] 18 Mar 2016

Implication of the 750 GeV diphoton resonance on two-Higgs-doublet model and its extensions with Higgs field

Xiao-Fang Han[1], Lei Wang[2,1]

[1] *Department of Physics, Yantai University, Yantai 264005, P. R. China*

[2] *IFIC, Universitat de València-CSIC,*

Apt. Correus 22085, E-46071 València, Spain

Abstract

We examine the implication of the 750 GeV diphoton resonance on the two-Higgs-doublet model imposing various theoretical and experimental constraints. The production rate of two-Higgs-doublet model is smaller than the cross section observed at the LHC by two order magnitude. In order to accommodate the 750 GeV diphoton resonance, we extend the two-Higgs-doublet model by introducing additional Higgs fields, and focus on two different extensions, an inert complex Higgs triplet and a real scalar septuplet. With the 125 GeV Higgs being agreement with the observed data, the production rate for the 750 GeV diphoton resonance can be enhanced to 0.6 fb for the former and 4.5 fb for the latter. The results of the latter are well consistent with the 750 GeV diphoton excess at the LHC.

PACS numbers: 12.60.Fr, 14.80.Ec, 14.80.Bn

I. INTRODUCTION

Very recently, the ATLAS and CMS collaborations have reported an excess of events in the diphoton channel with an invariant mass of about 750 GeV [1]. The local significance of this signal is at the 3σ level for ATLAS and slightly less for CMS. The approximate production cross section times branching ratio is 4.47±1.86 fb for CMS and 10.6±2.9 fb for ATLAS by the combination of 8 and 13 TeV data [2]. However, there are no excesses for the dijet [3], $t\bar{t}$ [4], diboson or dilepton channels, which gives a challenge to the the possible new physics model accommodating the 750 GeV diphoton resonance. Some plausible explanations of this excess have already appeared [2, 5–7]. The two-Higgs-doublet model (2HDM) can not produce the enough large cross section to accommodate the 750 GeV diphoton resonance. Ref. [7] introduces some additional vectors-like quarks and leptons to 2HDM in order to enhance the production rate of 750 GeV diphoton resonance.

In this paper, we first examine the implication of the 750 GeV diphoton resonance on the two-Higgs-doublet model imposing various theoretical and experimental constraints. We give the allowed mass ranges of the pseudoscalar and charged Higgs for $m_H = 750$ GeV, and find that the production rate of 2HDM is smaller than the cross section observed at the LHC by two order magnitude. Finally, in order to explain the 750 GeV diphoton excess, we extend the two-Higgs-doublet model by introducing additional Higgs fields, and focus on two different extensions, an inert complex Higgs triplet and a real scalar septuplet. We find that the production rate for the 750 GeV diphoton resonance can reach 0.6 fb for the former and 4.5 fb for the latter with the 125 GeV Higgs being consistent with the observed data.

Our work is organized as follows. In Sec. II we recapitulate the two-Higgs-doublet model. In Sec. III we introduce the numerical calculations, and examine the implications of the 750 GeV diphoton resonance on the 2HDM after imposing the theoretical and experimental constraints. In Sec. IV, we respectively add an inert complex Higgs triplet and a real scalar septuplet to 2HDM, and discuss the production rate for the 750 GeV diphoton resonance. Finally, we give our conclusion in Sec. V.

II. TWO-HIGGS-DOUBLET MODEL

The general Higgs potential is written as [8]

$$\begin{aligned}
\mathrm{V} \;=\; & m_{11}^2(\Phi_1^\dagger\Phi_1) + m_{22}^2(\Phi_2^\dagger\Phi_2) - \Big[m_{12}^2(\Phi_1^\dagger\Phi_2 + \mathrm{h.c.})\Big] \\
& + \frac{k_1}{2}(\Phi_1^\dagger\Phi_1)^2 + \frac{k_2}{2}(\Phi_2^\dagger\Phi_2)^2 + k_3(\Phi_1^\dagger\Phi_1)(\Phi_2^\dagger\Phi_2) + k_4(\Phi_1^\dagger\Phi_2)(\Phi_2^\dagger\Phi_1) \\
& + \left[\frac{k_5}{2}(\Phi_1^\dagger\Phi_2)^2 + \mathrm{h.c.}\right] + \Big[k_6(\Phi_1^\dagger\Phi_1)(\Phi_1^\dagger\Phi_2) + \mathrm{h.c.}\Big] \\
& + \Big[k_7(\Phi_2^\dagger\Phi_2)(\Phi_1^\dagger\Phi_2) + \mathrm{h.c.}\Big]\,. \qquad (1)
\end{aligned}$$

Here we focus on the CP-conserving case where all k_i and m_{12}^2 are real, and take $k_6 = k_7 = 0$. This can be realized by introducing a discrete Z_2 symmetry, and m_{12}^2 is a soft-breaking term. The two complex scalar doublets have the hypercharge $Y = 1$,

$$\Phi_1 = \begin{pmatrix} \phi_1^+ \\ \frac{1}{\sqrt{2}}\left(v_1 + \phi_1^0 + i a_1\right) \end{pmatrix}, \quad \Phi_2 = \begin{pmatrix} \phi_2^+ \\ \frac{1}{\sqrt{2}}\left(v_2 + \phi_2^0 + i a_2\right) \end{pmatrix}. \qquad (2)$$

Where the electroweak vacuum expectation values (VEVs) $v^2 = v_1^2 + v_2^2 = (246\ \mathrm{GeV})^2$, and the ratio of the two VEVs is defined as usual to be $\tan\beta = v_2/v_1$. After spontaneous electroweak symmetry breaking, there are five physical Higgses: two neutral CP-even h and H, one neutral pseudoscalar A, and two charged scalar $H^\pm$.

The general Yukawa interaction can be given as

$$\begin{aligned}
\mathcal{L}_Y \;=\; & \frac{-1}{\sqrt{2}}\bar{f}\left[z^f \sin(\beta-\alpha) + \rho^f \cos(\beta-\alpha)\right] h^0 f \\
& + \frac{-1}{\sqrt{2}}\bar{f}\left[z^f \cos(\beta-\alpha) - \rho^f \sin(\beta-\alpha)\right] H^0 P_R f + \frac{i}{\sqrt{2}}\,\mathrm{sign}(Q_f)\bar{f}\rho^f A^0 P_R f \\
& - \bar{u}\left[V\rho^d P_R - \rho^{u\dagger} V P_L\right] d H^+ - \bar{\nu}\left[\rho^\ell P_R\right]\ell H^+ + \mathrm{H.c.}. \qquad (3)
\end{aligned}$$

Where $f = u\ , d,\ \ell$, and $z^f = \sqrt{2}m_f/v$, while ρ matrices are free and have both diagonal and off-diagonal elements. For the aligned 2HDM [9], $\rho = \sqrt{2}m_f\kappa_f/v$, which leads that the couplings of neutral Higgs bosons normalized to the SM Higgs boson are give by

$$\begin{aligned}
& y_V^h = \sin(\beta-\alpha), \quad y_f^h = \sin(\beta-\alpha) + \cos(\beta-\alpha)\kappa_f, \\
& y_V^H = \cos(\beta-\alpha), \quad y_f^H = \cos(\beta-\alpha) - \sin(\beta-\alpha)\kappa_f, \\
& y_V^A = 0, \qquad y_u^A = -i\gamma^5\kappa_u, \qquad y_{d,\ell}^A = i\gamma^5\kappa_{d,\ell}. \qquad (4)
\end{aligned}$$

Where V denotes Z and W. We fix $\kappa_u = 1/\tan\beta$, which denotes that a special basis is taken where there is no the up-type quark coupling to Φ_1 [10, 11].

III. NUMERICAL CALCULATIONS AND RESULTS OF 2HDM

A. numerical calculations

We use 2HDMC [12] to implement the theoretical constraints from the vacuum stability, unitarity and coupling-constant perturbativity [13], and calculate the oblique parameters (S, T, U) and $\delta\rho$. HiggsBounds-4.1.4 [14, 15] is employed to implement the exclusion constraints from the neutral and charged Higgses searches at LEP, Tevatron and LHC at 95% confidence level. The in-house code is used to calculate the $B \to X_s\gamma$, Δm_{B_s}, and R_b. The experimental values of electroweak precision data, $B \to X_s\gamma$, Δm_{B_s} are taken from [16] and R_b from [17].

Since we focus on the implications of 750 GeV diphoton resonance on the 2HDM, we fix $m_h = 125$ GeV, $m_H = 750$ GeV, $|\sin(\beta-\alpha)| = 1$, $\kappa_d = \kappa_\ell$=0. The last three choices can naturally accommodate the non-observation of excesses for diboson, dijet and dilepton. We scan randomly the parameters in the following ranges:

$$\begin{aligned} &375 \text{ GeV} \leq m_{H^\pm} \leq 2000 \text{ GeV}, \\ &0.5 \leq \tan\beta \leq 5, \\ &-(2000 \text{ GeV})^2 \leq m_{12}^2 \leq (2000 \text{ GeV})^2. \end{aligned} \tag{5}$$

Since the heavy CP-even Higgs coupling to the top quark is proportional to $1/\tan\beta$ for $\cos(\beta-\alpha)$ =0, we take the small $\tan\beta$ to avoid the sizable suppression of this coupling. We take $m_A \simeq m_H$ which leads that the 750 GeV diphoton resonance is from both H and A, and the more large cross section may be obtained. We define

$$R_{\gamma\gamma} \equiv \sigma(gg \to H) \times Br(H \to \gamma\gamma) + \sigma(gg \to A) \times Br(A \to \gamma\gamma). \tag{6}$$

In this paper we will introduce additional Higgs fields to 2HDM, and some multi-charged scalars give very important contributions to the CP-even Higgs decay into $\gamma\gamma$. Therefore, we give the general formulas for the CP-even Higgs decay into $\gamma\gamma$ [18],

$$\Gamma(H \to \gamma\gamma) = \frac{\alpha^2 m_H^3}{256\pi^3 v^2} \left| \sum_i y_i N_{ci} Q_i^2 F_i \right|^2, \tag{7}$$

with N_{ci}, Q_i are the color factor and the electric charge respectively for particles running in the loop. The dimensionless loop factors for particles of spin given in the subscript are

$$F_1(\tau) = 2+3\tau+3\tau(2-\tau)f(\tau), \quad F_{1/2}(\tau) = -2\tau[1+(1-\tau)f(\tau)], \quad F_0(\tau) = \tau[1-\tau f(\tau)], \tag{8}$$

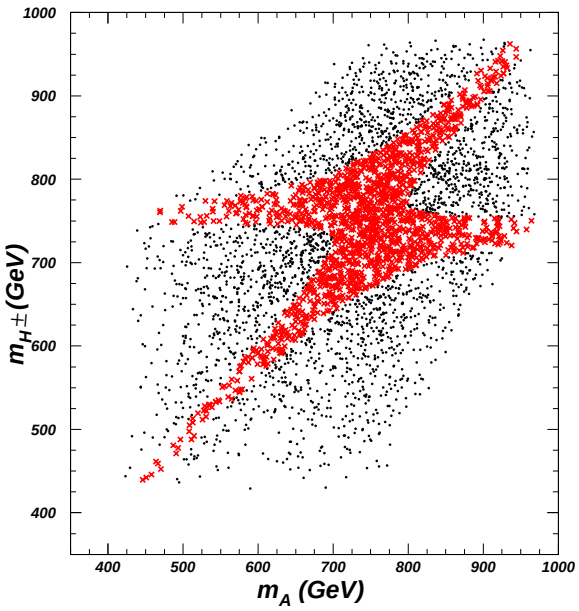

FIG. 1: The scatter plots of surviving samples projected on the planes of m_A versus $m_{H^\pm}$. All the samples are allowed by the theoretical constraints. The crosses (red) and bullets (black) are respectively allowed and excluded by the oblique parameters and $\Delta\rho$.

where $\tau = 4m_i^2/m_H^2$ and y_i is from

$$\mathcal{L} = -\frac{m_t}{v} y_t \bar{t}tH + 2\frac{m_W^2}{v} y_W W^+W^-H - 2\frac{m_\phi^2}{v} y_\phi \phi\phi H. \tag{9}$$

$$f(\tau) = \begin{cases} [\sin^{-1}(1/\sqrt{\tau})]^2, & \tau \geq 1 \\ -\frac{1}{4}[\ln(\eta_+/\eta_-) - i\pi]^2, & \tau < 1 \end{cases} \tag{10}$$

B. results and discussions

First we examine the allowed mass range of pseudoscalar and charged Higgs for $m_H = 750$ GeV after imposing the theoretical constraints, oblique parameters and $\Delta\rho$, where we scan m_A in the range of 375 GeV $\leq m_A \leq$ 2000 GeV. In Fig. 1, we project the surviving samples on the plane of m_A versus $m_{H^\pm}$. m_A and $m_{H^\pm}$ are favored in the range of 700 GeV and 800 GeV. In addition, the pseudoscalar and charged Higgs masses are allowed to have sizable deviations from 750 GeV for the small mass splitting between them. Also the pseudoscalar mass is allowed to have sizable deviation from 750 GeV for $m_{H^\pm}$ is around 750 GeV.

Now we calculate $R_{\gamma\gamma}$ taking $m_A \simeq m_H = 750$ GeV. Fig. 1 shows that $m_{H^\pm}$ is required to be larger than 650 GeV for $m_A \simeq m_H = 750$ GeV. For the decay $H \to \gamma\gamma$, the form factor

of scalar-loop is generally much smaller than that of fermion-loop. Further, $4m^2_{H^\pm}/m^2_H$ has sizable deviation from 1 where the peak of form factor appears. Therefore, the contribution of the charged Higgs to the decay $H \to \gamma\gamma$ is much smaller than that of top quark unless the top quark Yukawa coupling is sizably suppressed by a large $\tan\beta$. The W boson does not give the contribution to the decay $H \to \gamma\gamma$ since the H couplings to gauge bosons are zero for $\cos(\beta-\alpha)=0$. The decays $H \to H^+H^-,\ AA,\ AZ$ are kinematically forbidden, and the widths of $H \to\ WW,\ ZZ,\ b\bar{b},\ \tau\bar{\tau}$ are zero due to $\cos(\beta-\alpha)=0$ and $\kappa_d=\kappa_\ell=0$. Also the H coupling to hh is zero for $\cos(\beta-\alpha)=0$, and we will give the detailed explanation in the Appendix A. The width of $H \to H^\pm W^\mp$ can be comparable to $H \to t\bar{t}$ for the small charged Higgs mass. However, $m_{H^\pm}$ is required to be larger than 650 GeV, which leads the width to be sizably suppressed by the large phase space. Therefore, the decay $H \to t\bar{t}$ dominates the total width of the heavy Higgs.

In this paper we focus on the CP-conserving case where all the couplings constants of Higgs potential are taken to be real. Therefore, the pseudoscalar A coupling to hh is zero. The pseudoscalar has no decays $A \to WW,\ ZZ,\ hh$, and the widths of $A \to hZ,\ b\bar{b},\ \tau\bar{\tau}$ are zero due to $\cos(\beta-\alpha)=0$ and $\kappa_d=\kappa_\ell=0$. Therefore, $A \to t\bar{t}$ is the dominant decay channel. Since the charged Higgs and gauge boson do not give the contributions to $H \to \gamma\gamma$, the top quark plays the dominant contributions to $A \to \gamma\gamma$. In our calculations, we use 2HDMC to calculate the total widths of H and A including various possible decay channels.

In Fig. 2, we project the surviving samples on the planes of $R_{\gamma\gamma}$ versus $\tan\beta$ and $m_{H^\pm}$ versus $\tan\beta$. The left panel shows the $R_{\gamma\gamma}$ increases with decreasing of $\tan\beta$ since the $\sigma(gg \to H)$ and $\sigma(gg \to A)$ are proportional to $1/\tan^2\beta$, and the dependence $Br(H \to \gamma\gamma)$ and $Br(A \to \gamma\gamma)$ on $\tan\beta$ can be canceled to some extent by the widths of $t\bar{t}$ and $\gamma\gamma$ channels. However, due to the constraints of R_b, $B \to X_s\gamma$ and Δm_{B_s}, $\tan\beta$ is favored to be larger than 1, which leads that the maximal value of $R_{\gamma\gamma}$ is 0.015 fb. The correlations among $R_{\gamma\gamma}$, $\tan\beta$ and $m_{H^\pm}$ are shown in the right panel.

IV. EXTENDING 2HDM WITH ADDITIONAL HIGGS FIELD

In the minimal version of 2HDM, the production rate of 750 GeV diphoton resonance only can reach 0.015 fb, which is smaller than cross section observed by CMS collaboration

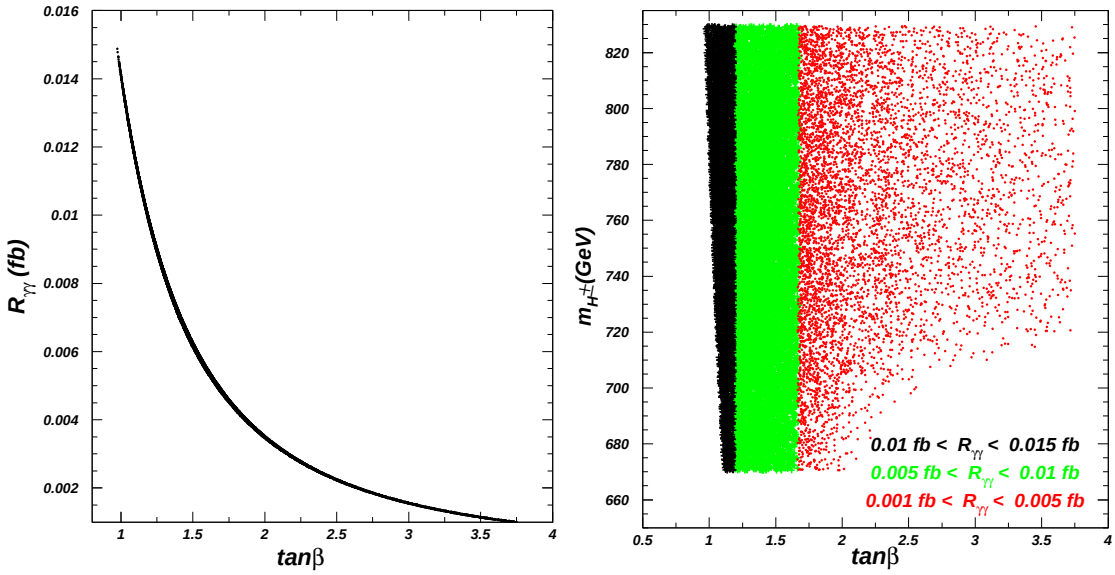

FIG. 2: The scatter plots of surviving samples projected on the planes of $R_{\gamma\gamma}$ versus $\tan\beta$ and $m_{H^\pm}$ versus $\tan\beta$.

by two order of magnitude. Ref. [7] introduces additional vector-like quark and lepton to 2HDM in order to enhance the production rate. Here we will extend 2HDM with additional Higgs fields and discuss two different extensions, an inert complex Higgs triplet and a real scalar septuplet.

A. 2HDM with an inert complex Higgs triplet (2HDM-IHT)

The extension SM with a complex Higgs triplet is proposed in [19], called type-II seesaw model, and ref. [20] also extends SM with an inert complex Higgs triplet. Here we add an inert complex $\mathrm{SU(2)_L}$ triplet scalar field Δ with $Y = 2$ to the 2HDM imposing an Z_2 symmetry in which the triplet is assigned to be odd and the others even. The VEV of triplet scalar field is zero to keep the Z_2 symmetry unbroken. The potential of triplet field is written as

$$\begin{aligned} V &= M^2 Tr(\Delta^\dagger\Delta) + \lambda_1 Tr(\Delta^\dagger\Delta)^2 + \lambda_2 (Tr\Delta^\dagger\Delta)^2 + \lambda_3 \Phi_1^\dagger \Delta\Delta^\dagger \Phi_1 + \lambda_4 (\Phi_1^\dagger\Phi_1) Tr(\Delta^\dagger\Delta) \\ &\quad + \lambda_3' \Phi_2^\dagger \Delta\Delta^\dagger \Phi_2 + \lambda_4' (\Phi_2^\dagger \Phi_2) Tr(\Delta^\dagger\Delta), \end{aligned} \tag{11}$$

where

$$\Delta = \begin{pmatrix} \delta^+/\sqrt{2} & \delta^{++} \\ (\delta_r^0 + i\delta_i^0)/\sqrt{2} & -\delta^+/\sqrt{2} \end{pmatrix}. \tag{12}$$

After the two Higgs doublet Φ_1 and Φ_2 acquire the VEVs, the last four terms in Eq. (11) will give the additional contributions to the masses of components in the triplet, respectively. At the tree-level, the Higgs triplet masses are given as,

$$\begin{aligned}
m^2_{\delta^{\pm\pm}} &= M^2 + \frac{1}{2}v^2(\lambda_4 c^2_\beta + \lambda'_4 s^2_\beta) \\
m^2_{\delta^{\pm}} &= M^2 + \frac{1}{2}v^2(\lambda_4 c^2_\beta + \lambda'_4 s^2_\beta) + \frac{1}{4}v^2(\lambda_3 c^2_\beta + \lambda'_3 s^2_\beta) \\
m^2_{\delta^0_r} &= m^2_{\delta^0_i} = M^2 + \frac{1}{2}v^2(\lambda_4 c^2_\beta + \lambda'_4 s^2_\beta) + \frac{1}{2}v^2(\lambda_3 c^2_\beta + \lambda'_3 s^2_\beta).
\end{aligned} \tag{13}$$

The charged Higgs triplet scalars couplings to the h and H are given as,

$$\begin{aligned}
h\delta^+\delta^- &: \; -\frac{1}{2}v\left(\lambda'_3 c_\alpha s_\beta - \lambda_3 s_\alpha c_\beta + 2\lambda'_4 c_\alpha s_\beta - 2\lambda_4 s_\alpha c_\beta\right) \\
H\delta^+\delta^- &: \; -\frac{1}{2}v\left(\lambda'_3 s_\alpha s_\beta + \lambda_3 c_\alpha c_\beta + 2\lambda'_4 s_\alpha s_\beta + 2\lambda_4 c_\alpha c_\beta\right) \\
h\delta^{++}\delta^{--} &: \; -v\left(\lambda'_4 c_\alpha s_\beta - \lambda_4 s_\alpha c_\beta\right) \\
H\delta^{++}\delta^{--} &: \; -v\left(\lambda'_4 s_\alpha s_\beta + \lambda_4 c_\alpha c_\beta\right).
\end{aligned} \tag{14}$$

B. 2HDM with a real scalar septuplet (2HDM-RSS)

The extension of SM with the complex and real scalar septuplet has been studied in [21] and [22]. Here we introduce a real scalar septuplet to the 2HDM assuming that the septuplet does not develop the VEV. The potential of the septuplet field Σ is written as

$$\begin{aligned}
V \;=\; & M^2\Sigma^\dagger\Sigma + \lambda_1(\Sigma^\dagger\Sigma)^2 + \frac{\lambda_2}{48}(\Sigma^\dagger T^a T^b \Sigma)^2 \\
& + \lambda_3(\Phi_1^\dagger\Phi_1)(\Sigma^\dagger\Sigma) + \lambda'_3(\Phi_2^\dagger\Phi_2)(\Sigma^\dagger\Sigma),
\end{aligned} \tag{15}$$

where

$$\Sigma = \frac{1}{\sqrt{2}}\left(T^{+++},\; T^{++},\; T^{+},\; T^0,\; T^-,\; T^{--},\; T^{---}\right)^T. \tag{16}$$

After the two Higgs doublet Φ_1 and Φ_2 develop the VEVs, the last two terms in Eq. (15) will give the additional contributions to the masses of all components of Σ. The septuplet scalars are degenerate at the tree-level and their mass are

$$m^2_\Sigma = M^2 + \frac{1}{2}v^2(\lambda_3 c^2_\beta + \lambda'_3 s^2_\beta). \tag{17}$$

The charged components of septuplet couplings to the h and H are,

$$\begin{aligned}
hT^+T^- = hT^{++}T^{--} = hT^{+++}T^{---} &: \; -v\left(\lambda'_3 c_\alpha s_\beta - \lambda_3 s_\alpha c_\beta\right) \\
HT^+T^- = HT^{++}T^{--} = HT^{+++}T^{---} &: \; -v\left(\lambda'_3 s_\alpha s_\beta + \lambda_3 c_\alpha c_\beta\right).
\end{aligned} \tag{18}$$

C. calculations and discussions

In the original 2HDM, the production rate for the 750 GeV diphoton resonance increases with decreasing of $\tan\beta$. However, the R_b and B flavor observables disfavor $\tan\beta$ to be smaller than 1. Therefore, in the following calculations we will take

$$\tan\beta = 1, \quad \sin(\beta-\alpha) = 1. \tag{19}$$

Further, in order to forbid the new charged Higgses altering the 125 GeV Higgs decay into $\gamma\gamma$ via one-loop effects, we require the light CP-even Higgs couplings to these charged Higgses to be zero, which leads for Eq. (19),

$$\lambda_4 = -\lambda_4' \text{ and } \lambda_3 = -\lambda_3' \text{ for 2HDM} - \text{IHT}, \tag{20}$$

$$\lambda_3 = -\lambda_3' \text{ for 2HDM} - \text{RSS}. \tag{21}$$

For Eq. (19) and Eq. (20), the triplet scalar masses in the 2HDM-IHT become degenerate,

$$m^2_{\delta^{\pm\pm}} = m^2_{\delta^{\pm}} = m^2_{\delta^0_r} = m^2_{\delta^0_i} = M^2. \tag{22}$$

The H couplings to the charged components of triplet are,

$$H\delta^+\delta^- : -\left(\lambda_4 + \frac{1}{2}\lambda_3\right)v, \qquad H\delta^{++}\delta^{--} : -\lambda_4 v. \tag{23}$$

Similarly, the septuplet scalar masses of the 2HDM-RSS are

$$m_\Sigma = M. \tag{24}$$

The H couplings to the charged components of septuplet are,

$$HT^+T^- = HT^{++}T^{--} = HT^{+++}T^{---} : \ -\lambda_3 v. \tag{25}$$

For the Higgs triplet and septuplet, the mass splitting among the components can be induced by loop corrections, and the charged components are very slightly heavier than the neutral components [20, 22]. These mass splittings are negligibly small, and the two extensions can be well consistent with the oblique parameters. Both the Higgs triplet and septuplet have no interactions with fermions, and the interactions with gauge bosons have to contain two components simultaneously, which makes them to be hardly constrained by the low energy observables and collider experimental searches. For the inert scalars, the

multi-lepton + $\not{E}_T$ is regarded as one of the most promising channels at the LHC. Taking the inert Higgs triplet model as an example, the charged scalars can be produced at the LHC through Drell-Yan process,

$$q\bar{q} \to \delta^+\delta^-,\ \delta^{++}\delta^{--},\ \delta^{\pm}\delta^{\mp\mp}, \tag{26}$$

and the charged scalars can have the following cascade decay assuming $m_{\delta^{\pm\pm}} > m_{\delta^\pm} > m_{\delta_i^0} > m_{\delta_r^0}$ (δ_r^0 is the stable particle),

$$\begin{aligned}
&\delta^{\pm\pm} \to \delta^\pm\ W^{\pm(*)}\ (W^{\pm(*)} \to l^\pm\ \nu),\\
&\delta^\pm \to W^{\pm(*)}\ \delta_r^0 \to l^\pm\ \nu\ \delta_r^0,\\
&\delta^\pm \to W^{\pm(*)}\ \delta_i^0 \to l^\pm\ \nu\ \delta_r^0\ Z^{(*)}\ (Z^{(*)} > l^\pm l^\mp).
\end{aligned} \tag{27}$$

The ATLAS and CMS collaborations have searched the $2l + \not{E}_T$ [23, 24], $3l + \not{E}_T$ [24, 25] and $4l + \not{E}_T$ [24], and set the limits on the next-to-lightest neutralino, the lightest-neutralino and chargino in the supersymmetric model. The lower bound of their masses can be up to hundreds of GeV for the large mass splittings. The ATLAS and CMS searches for the multi-lepton + $\not{E}_T$ signals rely on triggers that require $p_T > 20$ GeV for the transverse momentum of one lepton at least. The produced leptons tend to become soft with the decreasing of the mass splittings, and the soft leptons are difficult to be detected due to the lepton p_T requirements of the search. For example, using the $3l + \not{E}_T$ signal at the 14 TeV LHC, the 300 fb^{-1} of data is required to discover these supersymmetric spectra with dark mass between 40 GeV and 140 GeV for the mass splittings drop down to 9 GeV [26]. In this paper, the charged and neutral components of the inert scalar multiplets are degenerate at the tree-level, and the loop corrections only make the charged components to be very slightly heavier than the neutral components [20, 22]. For such small mass splitting, the leptons of the multi-lepton + $\not{E}_T$ event are very soft. Therefore, the inert scalars are free from the constraints of the ATLAS and CMS searches for the multi-lepton + $\not{E}_T$ at the 8 TeV LHC, and even difficult to be detected at the 14 TeV LHC with the more high integrated luminosity. Note that in order to enhance the 750 GeV Higgs decay into diphoton, in this paper we take the masses of the inert scalars to be in the range of 375 GeV and 500 GeV. Such range of mass will lead the relic density to be much smaller than the observed value although the lightest neutral component is stable [20]. Therefore, to produce the observed

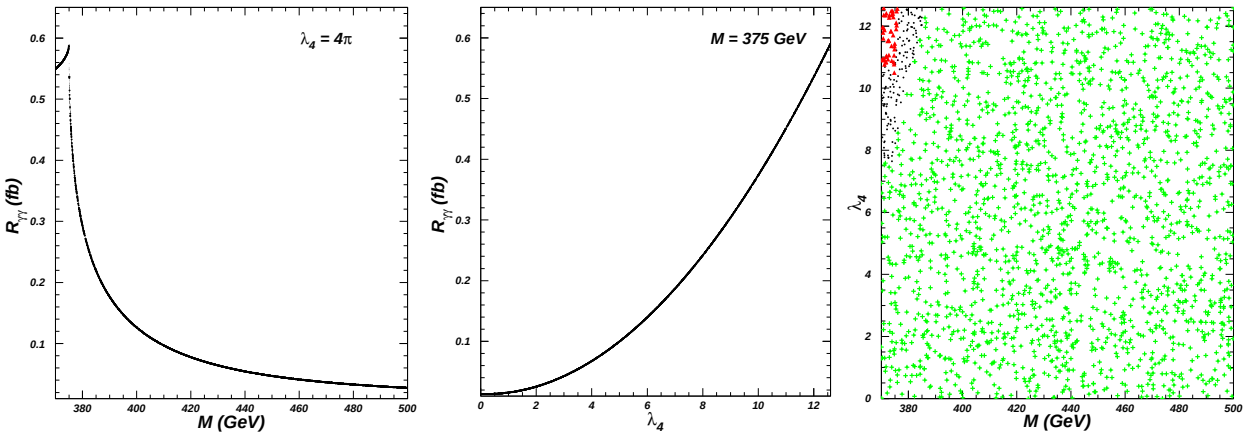

FIG. 3: $R_{\gamma\gamma}$ versus M, $R_{\gamma\gamma}$ versus λ_4 and λ_4 versus M in the 2HDM with an inert complex Higgs triplet. In the right panel $R_{\gamma\gamma} < 0.2$ fb for the pluses (green), 0.2 fb $< R_{\gamma\gamma} < 0.4$ fb for the bullets (black) and 0.4 fb $< R_{\gamma\gamma} < 0.6$ fb for the triangles (red).

relic density [27], some other dark matter sources need be introduced, which is beyond the scope of this paper.

For $\tan\beta = 1$ and $\sin(\beta-\alpha) = 1$, the H couplings to the charged Higgs $H^\pm$ of the original 2HDM is zero. Therefore, the $H^\pm$ does not give the contributions to the decay $H \to \gamma\gamma$. For 2HDM-IHT, the doubly charged and singly charged Higgses $\delta^{\pm\pm}$ and $\delta^\pm$ give additional contributions to the decay $H \to \gamma\gamma$, which are sensitive to the mass M and the coupling constants λ_4, λ_3. The degenerate masses of the triplet scalars are taken to be larger than 375 GeV, which makes the 750 GeV Higgs decays into triplet scalars to be kinematically forbidden. The perturbativity requires the absolute values of λ_4 and λ_3 in the quartic terms to be smaller than 4π. The stability of the potential favors λ_4 and λ_3 to be larger than 0, and gives the lower bound of λ_4 and λ_3 for they are smaller than zero [28]. Thus we take $0 < \lambda_4 < 4\pi$ and fix $\lambda_3 = 3$ [29]. Because $\delta^{\pm\pm}$ has an electric charge of ± 2, the $\delta^{\pm\pm}$ contributions are enhanced by a relative factor 4 in the amplitude of $H \to \gamma\gamma$, see Eq. (7), which can help $\delta^{\pm\pm}$ contributions dominate over the other particle contributions. Since there are the same sign between $H\delta^{++}\delta^{--}$ and $H\delta^+\delta^-$, the $\delta^{\pm\pm}$ and $\delta^\pm$ contributions are constructive each other.

In the Fig. 3, we project the samples of 2HDM-IHT on the planes of $R_{\gamma\gamma}$ versus M, $R_{\gamma\gamma}$ versus λ_4 and λ_4 versus M. The left panel shows that $R_{\gamma\gamma}$ has a peak around $M = 375$ GeV, and decreases rapidly with increasing of M. The characteristic is determined by the form factor $F_0(\tau)$ in the $H \to \gamma\gamma$. $R_{\gamma\gamma}$ can reach 0.6 fb for $M = 375$ GeV and $\lambda_4 = 4\pi$, but

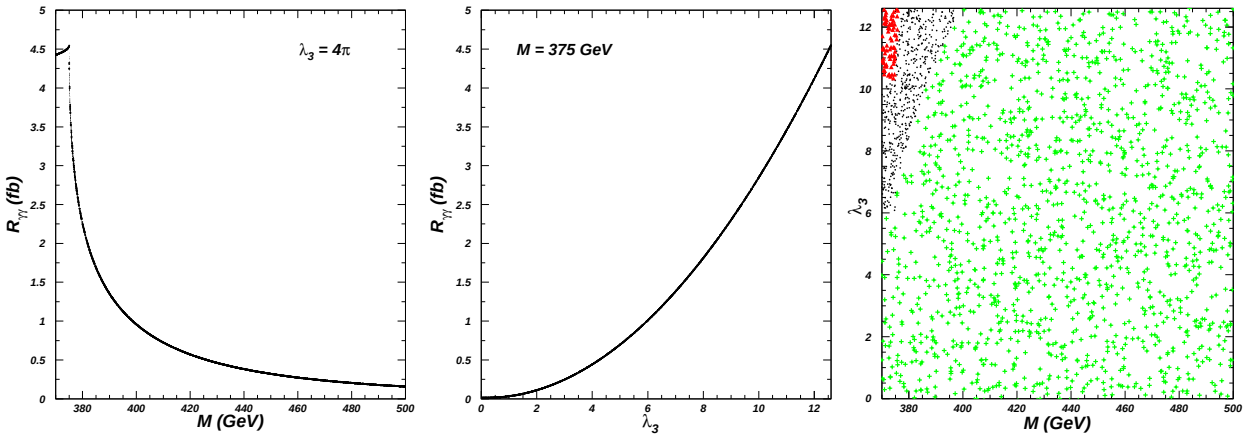

FIG. 4: $R_{\gamma\gamma}$ versus M, $R_{\gamma\gamma}$ versus λ_3 and λ_3 versus M in the 2HDM with a real scalar septuplet. In the right panel $R_{\gamma\gamma} < 1.0$ fb for the pluses (green), 1.0 fb $< R_{\gamma\gamma} <$ 3.0 fb for the bullets (black) and 3.0 fb $< R_{\gamma\gamma} <$ 4.6 fb for the triangles (red).

is still much smaller than the cross section for the 750 GeV diphoton resonance observed by CMS and ATLAS collaborations.

For the 2HDM-RSS, $T^{\pm\pm\pm}$, $T^{\pm\pm}$ and $T^{\pm}$ give additional contributions to the decay $H \to \gamma\gamma$, which are sensitive to the mass M and the coupling λ_3. The perturbativity requires the absolute value of λ_3 to be smaller than 4π, and $\lambda_3 > 0$ is free from the constraints of the potential stability [22]. Compared to the 2HDM-IHT, $T^{\pm\pm\pm}$ of 2HDM-RSS has an electric charge of ± 3, and the $T^{\pm\pm\pm}$ contributions are enhanced by a relative factor 9 in the amplitude of $H \to \gamma\gamma$, which makes $T^{\pm\pm\pm}$ contributions to dominate over the other particle contributions. Further, since there are the same sign between $HT^{+++}T^{---}$, $HT^{++}T^{--}$ and $HT^{+}T^{-}$, their contributions are constructive each other. Therefore, the width of $H \to \gamma\gamma$ of 2HDM-RSS can be much larger than that of 2HDM-ITH, approximate 8 times for the same Higgs coupling and mass. In the Fig. 4, we project the samples of 2HDM-RSS on the planes of $R_{\gamma\gamma}$ versus M, $R_{\gamma\gamma}$ versus λ_3 and λ_3 versus M. $R_{\gamma\gamma}$ can reach 4.6 fb for $M = 375$ GeV and $\lambda_3 = 4\pi$, which is approximate 8 times of the maximal value of of 2HDM-IHT. The right panel shows that $R_{\gamma\gamma} > 1$ fb favors $M < 400$ GeV and $\lambda_3 > 6$, and $R_{\gamma\gamma} > 3$ fb for $M < 380$ GeV and $\lambda_3 > 10$. Therefore, 2HDM-RSS can accommodate the 750 GeV diphoton resonance observed by the CMS and ATLAS at the LHC.

V. CONCLUSION

In this paper, we first consider various theoretical and experimental constraints, and examine the implications of the 750 GeV diphoton resonance on the two-Higgs-doublet model. We find the pseudoscalar and charged Higgs masses are favored in the range of 700 GeV and 800 GeV, and their masses are allowed to have sizable deviations from 750 GeV for the small mass splitting between them. Also the pseudoscalar mass is allowed to have sizable deviation from 750 GeV for the charged Higgs mass around 750 GeV. In the two-Higgs-doublet model, the production rate for 750 GeV diphoton resonance is smaller than the cross section observed at LHC by two order magnitude. In order to accommodate the 750 GeV diphoton resonance, we respectively introduce an inert complex Higgs triplet and a real scalar septuplet to the two-Higgs-doublet model. The multi-charged scalars in these models can enhance the branching ratio of $H \to \gamma\gamma$ sizably. The production rate for the 750 GeV diphoton resonance can be enhanced to 0.6 fb for 2HDM with an inert Higgs triplet and 4.5 fb for 2HDM with a real scalar septuplet. The latter can give a valid explanation for the 750 GeV diphoton resonance at the LHC.

Acknowledgment

This work has been supported in part by the National Natural Science Foundation of China under grant No. 11575152, and by the Spanish Government and ERDF funds from the EU Commission [Grants No. FPA2014-53631-C2-1-P, SEV-2014-0398, FPA2011-23778].

Appendix A: The coupling of Hhh

The scalar potential shown in the Eq. (1) is expressed in the physical basis where both Φ_1 and Φ_2 have the non-zero VEVs. It is more convenient to understand the coupling Hhh in the Higgs basis where the two scalar doublets are given as

$$H_1 = \begin{pmatrix} G^+ \\ \frac{1}{\sqrt{2}}\left(v+\rho_1+iG_0\right) \end{pmatrix} \equiv \Phi_1 c_\beta + \Phi_2 s_\beta\,, \quad H_2 = \begin{pmatrix} H^+ \\ \frac{1}{\sqrt{2}}\left(\rho_2+iA\right) \end{pmatrix} \equiv -\Phi_1 s_\beta + \Phi_2 c_\beta\,. \quad \text{(A1)}$$

In the Higgs basis, the H_1 field has a VEV v =246 GeV, and the VEV of H_2 field is zero.

The scalar potential in the physical basis (as shown in the Eq. (1)) can be expressed in the Higgs basis [30],

$$\begin{aligned}\mathcal{V} \;=\; & Y_1 H_1^\dagger H_1 + Y_2 H_2^\dagger H_2 + Y_3[H_1^\dagger H_2 + \text{h.c.}] + \tfrac{1}{2} Z_1 (H_1^\dagger H_1)^2 + \tfrac{1}{2} Z_2 (H_2^\dagger H_2)^2 + Z_3 (H_1^\dagger H_1)(H_2^\dagger H_2) \\ & + Z_4 (H_1^\dagger H_2)(H_2^\dagger H_1) + \left\{ \tfrac{1}{2} Z_5 (H_1^\dagger H_2)^2 + \left[Z_6 (H_1^\dagger H_1) + Z_7 (H_2^\dagger H_2) \right] H_1^\dagger H_2 + \text{h.c.} \right\}, \qquad \text{(A2)}\end{aligned}$$

where the Y_i are real linear combinations of the m_{ij}^2 and the Z_i are real linear combinations of the λ_i. For $\lambda_6 = \lambda_7 = 0$, we simply have [30]

$$\begin{aligned} Z_1 \;&\equiv\; \lambda_1 c_\beta^4 + \lambda_2 s_\beta^4 + \tfrac{1}{2} \lambda_{345} s_{2\beta}^2 \,, && \text{(A3)} \\ Z_2 \;&\equiv\; \lambda_1 s_\beta^4 + \lambda_2 c_\beta^4 + \tfrac{1}{2} \lambda_{345} s_{2\beta}^2 \,, && \text{(A4)} \\ Z_i \;&\equiv\; \tfrac{1}{4} s_{2\beta}^2 \big[\lambda_1 + \lambda_2 - 2\lambda_{345} \big] + \lambda_i \,, \quad (\text{for } i = 3, 4 \text{ or } 5) \,, && \text{(A5)} \\ Z_6 \;&\equiv\; -\tfrac{1}{2} s_{2\beta} \big[\lambda_1 c_\beta^2 - \lambda_2 s_\beta^2 - \lambda_{345} c_{2\beta} \big] \,, && \text{(A6)} \\ Z_7 \;&\equiv\; -\tfrac{1}{2} s_{2\beta} \big[\lambda_1 s_\beta^2 - \lambda_2 c_\beta^2 + \lambda_{345} c_{2\beta} \big] \,, && \text{(A7)} \end{aligned}$$

where $c_{2\beta} = \cos 2\beta$, $s_{2\beta} = \sin 2\beta$ and $\lambda_{345} = \lambda_3 + \lambda_4 + \lambda_5$.

The H^+ and A are the mass eigenstates of the charged Higgs boson and CP-odd Higgs boson, and their masses are given by

$$\begin{aligned} m_{H^+}^2 \;&=\; Y_2 + \tfrac{1}{2} Z_3 v^2 \,, \\ m_A^2 \;&=\; Y_2 + \tfrac{1}{2} (Z_3 + Z_4 - Z_5) v^2 . \end{aligned} \qquad \text{(A8)}$$

The physical CP-even Higgs bosons h and H are the linear combination of ρ_1 and ρ_2,

$$\begin{aligned} H \;&=\; \rho_1 \cos(\beta - \alpha) - \rho_2 \sin(\beta - \alpha), \\ h \;&=\; \rho_1 \sin(\beta - \alpha) + \rho_2 \cos(\beta - \alpha). \end{aligned} \qquad \text{(A9)}$$

For $\cos(\beta - \alpha) = 0$, there is no mixing of h and H, which requires $Z_6 = 0$ and leads to

$$H = -\rho_2, \qquad h = \rho_1. \qquad \text{(A10)}$$

For the Eq. (A10), the other terms except for the Z_6 term in the Eq. (A2) do not produce the coupling of Hhh. Therefore, the H coupling to hh is zero for $\cos(\beta - \alpha) = 0$.

Note that $\cos(\beta - \alpha)$ denotes the coupling of H and gauge bosons normalized to SM Higgs. Both $\cos(\beta - \alpha)$ and the coupling of Hhh are the physical observables and basis-independent. Therefore, for $\cos(\beta - \alpha) = 0$, the coupling of Hhh equals to zero in the

physical basis and Higgs basis. In fact, in the physical basis, the Higgs potential shown in Eq. (1) gives the coupling of Hhh [30],

$$g_{Hhh} = -\frac{\cos(\beta-\alpha)}{v}\Big\{4\overline{m}^2 - m_H^2 - 2m_h^2 \\ +2(3\overline{m}^2 - m_H^2 - 2m_h^2)[\sin(\beta-\alpha)\cot 2\beta - \cos(\beta-\alpha)]\cos(\beta-\alpha)\Big\}, \quad \text{(A11)}$$

with $\overline{m}^2 = m_A^2 + Z_5 v^2 + \frac{1}{2}(Z_6 - Z_7)\tan 2\beta v^2$. Where Z_5, Z_6 and Z_7 can be expressed using the coupling constants of Higgs potential in the physical basis according to Eq. (A5), Eq. (A6) and Eq. (A7). The Eq. (A11) explicitly shows that the coupling of Hhh equals to zero for $\cos(\beta-\alpha) = 0$ in the physical basis.

---

[1] ATLAS and CMS Collaborations - Dec. 15th talks by Jim Olsen and Marumi Kado, ATLAS and CMS physics results from Run 2, https://indico.cern.ch/event/442432/.

[2] S. D. Chiara, L. Marzola, M. Raidal, arXiv:1512.04939.

[3] V. Khachatryan et al. [CMS Collaboration], arXiv:1512.01224.

[4] V. Khachatryan et al. [CMS Collaboration], arXiv:1506.03062.

[5] K. Harigaya, Y. Nomura, arXiv:1512.04850; Y. Mambrini, G. Arcadi, A. Djouadi, arXiv:1512.04913; M. Backovic, A. Mariotti, D. Redigolo, arXiv:1512.04917; Y. Nakai, R. Sato, K. Tobioka, arXiv:1512.04924; S. Knapen, T. Melia, M. Papucci, K. Zurek, arXiv:1512.04928; D. Buttazzo, A. Greljo, D. Marzocca, arXiv:1512.04929; A. Pilaftsis, arXiv:1512.04931; R. Franceschini, G. F. Giudice, J. F. Kamenik, M. Mc- Cullough, A. Pomarol, R. Rattazzi, M. Redi, F. Riva, A. Strumia, R. Torre, arXiv:1512.04933; T. Higaki, K. S. Jeong, N. Kitajima, F. Takahashi, arXiv:1512.05295; S. D. McDermott, P. Meade, H. Ramani, arXiv:1512.05326; J. Ellis, S. A. R. Ellis, J. Quevillon, V. Sanz, T. You, arXiv:1512.05327; M. Low, A. Tesi, L.-T. Wang, arXiv:1512.05328; B. Bellazzini, R. Franceschini, F. Sala, J. Serra, arXiv:1512.05330; R. S. Gupta, S. Jger, Y. Kats, G. Perez, E. Stamou, arXiv:1512.05332; C. Petersson, R. Torre, arXiv:1512.05333; E. Molinaro, F. Sannino, N. Vignaroli, arXiv:1512.05334.

[6] B. Dutta, Y. Gao, T. Ghosh, I. Gogoladze, T. Li, arXiv:1512.05439; Q.-H. Cao, Y. Liu, K.-P. Xie, B. Yan, D.-M. Zhang, arXiv:1512.05542; S. Matsuzaki, K. Yamawaki, arXiv:1512.05564; A. Kobakhidze, F. Wang, L. Wu, J. M. Yang, M. Zhang, arXiv:1512.05585; R. Martinez, F. Ochoa, C.F. Sierra, arXiv:1512.05617; P. Cox, A. D. Medina, T. S. Ray, A. Spray,

arXiv:1512.05618; J. M. No, V. Sanz, J. Setford, arXiv:1512.05700; S. V. Demidov, D. S. Gorbunov, arXiv:1512.05723; W. Chao, R. Huo, J.-H. Yu, arXiv:1512.05738; S. Fichet, G. v. Gersdorff, C. Royon, arXiv:1512.05751; D. Curtin, C. B. Verhaaren, arXiv:1512.05753; L. Bian, N. Chen, D. Liu, J. Shu, arXiv:1512.05759; J. Chakrabortty, A. Choudhury, P. Ghosh, S. Mondal, T. Srivastava, arXiv:1512.05767; A. Ahmed, B. M. Dillon, B. Grzadkowski, J. F. Gunion, Y. Jiang, arXiv:1512.05771; P. Agrawal, J. Fan, B. Heidenreich, M. Reece, M. Strassler, arXiv:1512.05775; C. Csaki, J. Hubisz, J. Terning, arXiv:1512.05776; A. Falkowski, O. Slone, T. Volansky, arXiv:1512.05777; D. Aloni, K. Blum, A. Dery, A. Efrati, Y. Nir, arXiv:1512.05778; Y. Bai, J. Berger, R. Lu, arXiv:1512.05779; F. Wang, L. Wu, J. M. Yang, M. Zhang, arXiv:1512.06715; J. Cao, C. Han, L. Shang, W. Su, J. M. Yang, Y. Zhang, arXiv:1512.06728; J. J. Heckman, arXiv:1512.06773; J. Chang, K. Cheung, C.-T. Lu, arXiv:1512.06671; D. Becirevic, E. Bertuzzo, O. Sumensari, R. Z. Funchal, arXiv:1512.05623; A. Alves, A. G. Dias, K. Sinha, arXiv:1512.06091.

[7] A. Angelescu, A. Djouadi, G. Moreau, arXiv:1512.04921.

[8] R. A. Battye, G. D. Brawn, A. Pilaftsis, JHEP **1108**, 020 (2011).

[9] A. Pich, P. Tuzon, Phys. Rev. D **80**, 091702 (2009).

[10] W. Altmannshofer, S. Gori and G. D. Kribs, Phys. Rev. D **86**, 115009 (2012).

[11] V. Barger, L. L. Everett, H. E. Logan, G. Shaughnessy, Phys. Rev. D **88**, 115003 (2013).

[12] D. Eriksson, J. Rathsman, O. Stål, Comput. Phys. Commun. **181**, 189-205 (2010); Comput. Phys. Commun. **181**, 833-834 (2010).

[13] B. Grinstein, C. W. Murphy, P. Uttayarat, arXiv:1512.04567.

[14] P. Bechtle, O. Brein, S. Heinemeyer, G. Weiglein, K. E. Williams, Comput. Phys. Commun. **181**, 138-167 (2010).

[15] P. Bechtle, O. Brein, S. Heinemeyer, O. Stål, T. Stefaniak, G. Weiglein, K. E. Williams, Eur. Phys. Jour. C **74**, 2693 (2014).

[16] K. A. Olive etal. [Particle Data Group], Chin. Phys. C **38**, 090001 (2014).

[17] K. Nakamura et al. [Particle Data Group], J. Phys. G **37**, 075021 (2010).

[18] A. Djouadi, Phys. Rept. **459**, 1 (2008).

[19] W. Konetschny, W. Kummer, Phys. Lett. B **70**, 433 (1977); J. Schechter, J. W. F. Valle, Phys. Rev. D **22**, 2227 (1980); T. P. Cheng, L. F. Li, Phys. Rev. D **22**, 2860 (1980).

[20] T. Araki, C.Q. Geng, K. I. Nagao, Phys. Rev. D **83**, 075014 (2011).

[21] T. Hambye, F.-S. Ling, L. Lopez Honorez, J. Rocher, JHEP **0907**, 090 (2009) [Erratum-ibid. 1005, 066 (2010)]; F. S. Ling, arXiv:0905.4823; K. Earl, K. Hartling, H. E. Logan, T. Pilkington, Phys. Rev. D **88**, 015002 (2013); C. Garcia-Cely, A. Ibarra, A. S. Lamperstorfer, M. H. G. Tytgat, arXiv:1507.05536; L. Wang, X.-F. Han, Phys. Rev. D **87**, 015015 (2013); Phys. Rev. D **86**, 095007 (2012); Y. Cai, W. Chao, S. Yang, JHEP **1212**, 043 (2012); Y. Hamada, K. Kawana, K. Tsumura, Phys. Lett. B **747**, 238 (2015).

[22] C. Cai, Z.-M. Huang, Z. Kang, Z.-H. Yua, H.-H. Zhang, Phys. Rev. D **92**, 115004 (2015).

[23] ATLAS collaboration, JHEP **1405**, 071 (2014).

[24] CMS collaboration, Eur. Phys. Jour. C **74**, 3036 (2014).

[25] ATLAS collaboration, JHEP **1404**, 169 (2014).

[26] M. van Beekveld, W. Beenakker, S. Caron, R. R. de Austri, arXiv:1602.00590.

[27] P. A. R. Ade et al. [Planck Collaboration], Astron. Astrophys. **571**, A16 (2014).

[28] A. Arhrib, R. Benbrik, M. Chabab, G. Moultaka, M. C. Peyranere, L. Rahili, J. Ramadan, Phys. Rev. D **84**, 095005 (2011).

[29] A. Arhrib, R. Benbrik, M. Chabab, G. Moultaka, L. Rahili, JHEP **1204**, 136 (2012).

[30] J. Bernon, J. F. Gunion, H. E. Haber, Y. Jiang, S. Kraml, Phys. Rev. D **92**, 075004 (2015).